RSC Advances

PAPER

View Article Online
View Journal | View Issue

Cite this: *RSC Adv.*, 2015, **5**, 88973

An annealing-free anatase TiO_2 nanocrystal film as an electron collection layer in organic solar cells†

Di Li,[a] Yanli Chen,[b] Peng Du,[ab] Zhao Zhao,[a] Haifeng Zhao,[a] Yuejia Ma[a] and Zaicheng Sun*[a]

Received 21st August 2015
Accepted 14th October 2015

DOI: 10.1039/c5ra16932a

www.rsc.org/advances

Anatase TiO_2 film, which is traditionally fabricated by high-temperature annealing of TiO_x precursors, has been widely used as an electron collection layer in photovoltaics. In order to avoid the undesired high temperature treatment, in this work, we developed a convenient and moderate procedure to fabricate anatase TiO_2 nanocrystal films at room temperature. Ultrafine, clean and high-quality anatase TiO_2 nanocrystals have been pre-prepared in a simple solvothermal route and subsequent spin-coating of the nanocrystal dispersion provides a well formed TiO_2 nanocrystal film without any further thermal treatment. The characteristics of the TiO_2 nanocrystal film, in terms of crystallization phase, film morphology, optical and electronic properties, have been carefully studied, and then a typical [ITO/TiO_2/P3HT:PCBM/MoO_3/Ag] inverted photovoltaic device using TiO_2 nanocrystals as the ECL has been fabricated and exhibits a comparable power conversion efficiency (PCE) of 3.35% to that of the conventional device (3.39% PCE).

Introduction

Organic solar cells (OSCs) have attracted much attention in recent years because of their appealing advantages of low cost, light weight and mechanical flexibility compared with conventional silicon solar cells.[1–5] In order to improve the performances and stabilities of OSCs, besides elegantly optimizing the material systems and nanoscale phase separations, effectively collecting the charge carriers should also be focused on.[6–8] Indeed, electron collection layers play a crucial role in influencing the device performance for their energy-aligning capabilities, and of the reported ECLs, anatase TiO_2 is very attractive for its high environmental stability, suitable energy levels and high electron mobility.[9–15]

The most common approach to fabricate anatase TiO_2 ECL is high-temperature annealing (above 400 °C) to thoroughly transform amorphous TiO_x precursors into anatase TiO_2 (Scheme 1).[9,16] Apparently, the annealing process complicates the device fabrication and limits the applications in thermal sensitive substrates. In order to overcome this defect, several approaches have been developed to construct TiO_2 ECLs in mild conditions, such as atomic layer deposition, electrochemical deposition, electrospray, high-pressure crystallization, chemical vapor deposition, chemical sintering and nanocomposites.[17–22] However, these methods require either strict experimental conditions or complex TiO_x sol–gel precursors, thus restrain the availability and simplicity of device processing. Therefore, it remains a great challenge for exploring a highly efficient and convenient approach to fabricate high-quality anatase TiO_2 film as ECL in thin film photovoltaics at low temperature.

For common high-temperature annealing method, the essential phase transition to obtain anatase TiO_2 film was achieved above 400 °C and herein, we envisioned that the pre-prepared anatase TiO_2 followed by filming could avoid the undesired high temperature treatment (Scheme 1). Recently it has been reported that the nanocrystal layer of ultrafine n-type

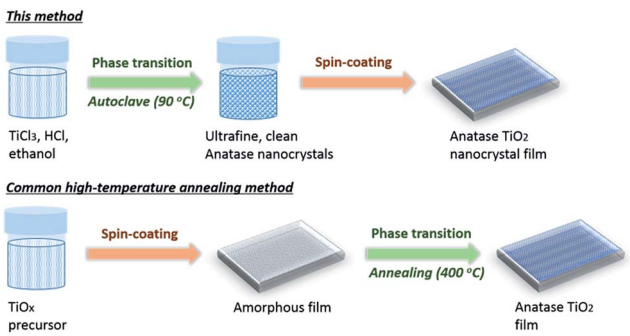

Scheme 1 Illustration of the approach in this work and common high-temperature annealing method to fabricate anatase TiO_2 film as ECL for photovoltaics.

[a]State Key Laboratory of Luminescence and Applications, Fine Mechanics and Physics, Chinese Academy of Sciences, 3888 East Nanhu Road, Changchun, Jilin 130033, P. R. China. E-mail: sunzc@ciomp.ac.cn

[b]Institute for New Energy Materials & Low-Carbon Technologies, School of Materials Science and Engineering, Tianjin University of Technology, Tianjin 300384, P. R. China

† Electronic supplementary information (ESI) available: Additional figures of HRTEM, AFM, UPS, SCLC and UV-Vis absorption. See DOI: 10.1039/c5ra16932a

semiconductor ZnO could serve as effective electron collection layer in perovskite solar cells.[23] Moreover, Snaith's group[24] and Boyen's group[25] separately reported similar approaches to fabricate nanocrystal TiO_2 films as ECLs. However, due to the large size of TiO_2 nanoparticles (diameter of around 4.5 nm and 6 nm, respectively), the addition of TiAcAc served as "electronic glue" and annealing at 135–150 °C to decompose TiAcAc to TiO_x and remove organic impurities were essential to fill the gaps between the large nanoparticle. In this work, we developed a convenient and moderate procedure to synthesize ultrafine (with diameter around 2–3 nm) and high-quality anatase TiO_2 nanocrystals without any additional surfactants or binders; then simply spin-coat the nanocrystal dispersion to give high-quality anatase TiO_2 nanocrystal film as ECL without any further treatments (Scheme 1). Finally, the utilization of this new approach was strongly indicated by efficient inverted OSCs.

Experimental section

Materials

$TiCl_3$ (15.0–20.0% basis in 30% HCl) and tetrabutyl titanate were purchased from Aladdin. Other chemicals used for synthesis were purchased from Beijing Chemical Works. P3HT and PCBM were purchased from Rieke Metals and Nano-C respectively and used as received. 1,2-Dichlorobenzene was purchased from Sigma-Aldrich and used without further purification.

Synthesis of TiO_2 nanocrystals

The anatase TiO_2 nanocrystals were synthesized in a facile and moderate procedure: the mixture of $TiCl_3$ (15–20%, 2 mL) and HCl (6 mol L^{-1}, 2 mL) in ethanol (30 mL) was heated at 90 °C for 6 h in an autoclave, followed by aging at room temperature for one week without further treatment. Before use, the TiO_2 nanoparticle dispersion was filtered through a 0.8 μm nylon syringe filter.

Preparation of nanocrystal TiO_2 film

The TiO_2 layer was obtained by spin-coating the dispersion of TiO_2 nanocrystals in ethanol at 2000 rpm for 1 min on ITO substrate and dried in air for 1 hour. The thickness of this TiO_2 layer in this spin-coating condition was estimated to be about 25–30 nm from the FE-SEM cross-section images (inset of Fig. 2a) and could be varied systematically by changing the spin-coating parameters or repeating the spin-coating process several times as needed.

Preparation of annealed TiO_2 film

4 mL tetrabutyl titanate was dissolved in 2 mL isopropanol in a conical flask for 5 min. 210 μL water and 17 μL concentrated HCl were mixed with 4 mL isopropanol for 5 min, then this solution was dropped into the conical flask over about 10 min, and the mixture was stirred for 12 h at room temperature. Before use, the resultant TiO_x precursor was diluted with isopropanol in the volume ratio of 1 : 3. The diluted solution was filtered through a 0.8 μm nylon syringe filter and then spin-coated (4000 rpm for 1 min) on ITO substrate and annealed at 400 °C for 30 min.

Device fabrication

The ITO glasses (~20 Ω cm^{-2}) were ultrasonically cleaned in detergent, deionized water, acetone and isopropyl alcohol. After routine solvent cleaning, the substrates were treated by O_2 plasma for 10 min. The TiO_2 layer (nanocrystal TiO_2 layer or annealed TiO_2 layer) was obtained by spin-coating without or with high temperature annealing as discussed before. Following that, an active layer was deposited on top of the TiO_2 layer by spin-coating a solution of the P3HT and PCBM blend with a weight ratio of 1 : 1 in 1,2-dichlorobenzene (40 mg mL^{-1}) at 700 rpm for 60 s in N_2 environment. The active layer was then dried in covered glass Petri dishes for 1 hour without further thermal annealing. Finally, a MoO_3 layer (5.5 nm) and an Ag layer (70 nm) were deposited by vacuum thermal evaporation and a metal shadow mask was used to define the device area of 5 mm^2. The current density–voltage (*J–V*) characteristics of the devices were measured in air using a Keithley 2400 parameter analyzer under a simulated light (AM 1.5G) with intensity of 100 mW cm^{-2}.

Characterizations

X-ray diffraction (XRD) study was performed on Bruker AXS D8 Focus apparatus using Cu Ka radiation (λ = 1.54056 Å). Ultraviolet photoelectron spectroscopy (UPS) spectra were recorded using a PREVAC XPS/UPS System under He irradiation ($h\nu$ = 21.2 eV). The transmittance of the TiO_2 films (on ITO/glass) was characterized using an UV-3600 Shimadzu UV-Vis-NIR spectrophotometer. Field emission scanning electron microscope (FE-SEM) images were measured on a JEOL JSM 4800F. Transmission electron microscope (TEM) images were taken using an FEI Tecnai G2 operated at 200 kV. The atomic force microscopy (AFM) measurements were performed on an S II Nanonavi probe station 300 HV (Seiko, Japan) in contact mode.

Results and discussion

TiO_2 nanoparticles were synthesized in a mild and facile procedure without any additional surfactants or binders. The morphologies of the resulted TiO_2 nanoparticles were characterized by TEM measurement. As shown in Fig. 1a, ultrafine and homogeneous TiO_2 nanoparticles were obtained by this method and the sizes distributed mainly in the range of 2–3 nm (inset of Fig. 1a), which were quite essential for fabricating high-quality TiO_2 film by spin-coating (*vide infra*). The crystalline phase of TiO_2 nanoparticles was determined carefully by HRTEM and XRD measurements. As shown in the inset of Fig. 1b, the apparent lattice fringes (d_{200} = 0.19 nm) on the particles revealed the anatase crystallization[26] and the assembled nanoparticles on the substrate exhibited continuous crystalline regions (Fig. S1 in ESI†), which proved a good crystallinity degree of the nanoparticle assembled film. Meanwhile, the XRD pattern (Fig. 1b) of the TiO_2 nanocrystal film confirmed that the film was composed of small size anatase nanocrystals due to the

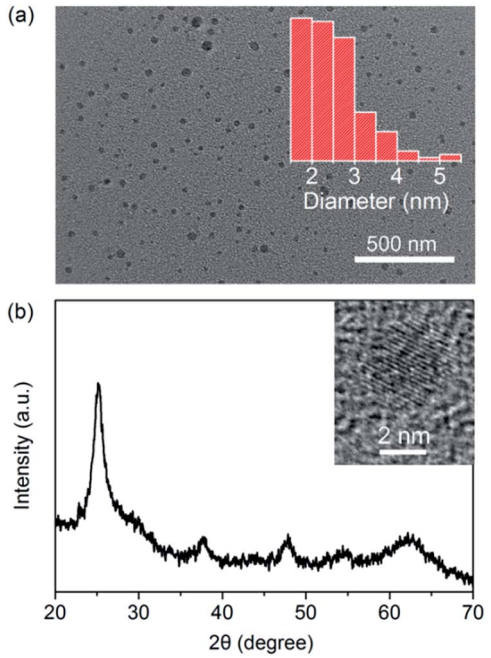

Fig. 1 (a) TEM image of the TiO_2 nanoparticles. Inset shows the size distribution histogram (155 particles measured), (b) XRD pattern of the anatase TiO_2 nanocrystals. Inset is HRTEM crystalline lattice fringes.

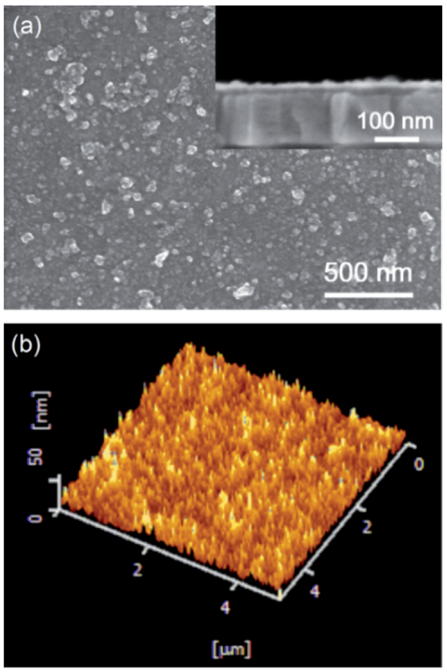

Fig. 2 (a) Top view and cross-section (inset) FE-SEM images of the TiO_2 nanocrystal film. (b) AFM image of the TiO_2 nanocrystal film.

widened standard anatase diffraction peaks (JCPDS no. 21-1272). It should be noted that the anatase TiO_2 nanocrystals prepared by this method were dispersed well in ethanol to form transparent colloid solution without any additional surfactants or binders which were undesired for fabricating high-quality TiO_2 layer because they would bring organic impurities and needed thermal decomposition to remove. This character combining with the advantage of ultrafine sizes of the TiO_2 nanoparticles enabled us to fabricate a transparent and compact TiO_2 layer by simply spin-coating the nanocrystal dispersion. It should be highlighted that the TiO_2 layer produced by this method was already pre-crystallized to anatase phase and able to directly apply as ECL in thin film photovoltaics without further crystallization treatments involving of annealing step. In order to study the advantages of the room-temperature processed nanocrystal TiO_2 layer as ECL in depth, conventional TiO_2 layer which was deposited from TiO_x sol–gel and then annealed at 400 °C to obtain anatase phase was prepared on ITO substrate for comparison.

The morphology of the spin-coated anatase TiO_2 nanocrystal film was studied by FE-SEM and AFM measurements. In the FE-SEM images (Fig. 2a), tiny nanocrystals assembled tightly to form compact layer. Because of the ultrafine size of the nanocrystals, interspaces between neighbouring particles could be drastically avoided to consolidate the film and benefit the electrical contact to electron transport. Both the top view and cross-section FE-SEM images (Fig. 2a) showed that the nanocrystal TiO_2 film was compact with no visible cracks or porosity, providing the important foundation for this film to serve as ECL. There were partial raised clusters on the nanocrystalline film surface and the AFM measurement revealed that the root mean square (RMS) surface roughness of the film was 5.77 nm (Fig. 2b), which was obviously higher than that of the conventional high-temperature annealed TiO_2 film (0.98 nm, Fig. S2 in ESI†). The higher roughness derived from the nanoparticle assembled surface could enhance the TiO_2/active layer interfacial surface area, which might be benefit to the carrier collection at the interface of ECL and active layer with shorter electron–hole diffusion lengths comparing with the film thickness.[27–29]

The optical transmittance spectra of various TiO_2 films on ITO substrates, including nanocrystalline TiO_2/ITO prepared by this method, conventional high-temperature annealed TiO_2/ITO and bare ITO, were compared (Fig. 3), and the thickness of the TiO_2 films on ITO was consistent with that in the optimized

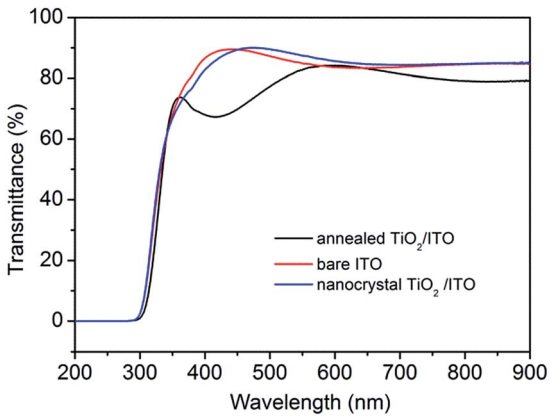

Fig. 3 Optical transmittance spectra of nanocrystal and annealed TiO_2 films on ITO substrates.

OSCs. Compared with bare ITO, the TiO_2 nanocrystal film could decrease the transmittance of ultraviolet light (350–400 nm) and enhance the transmittance beyond 450 nm. The decrease of transmittance in the ultraviolet region was caused by the absorption of the nanocrystal TiO_2 film (Fig. S3 in ESI†). This feature could protect the active layer from UV radiation and simultaneously enhance the transmittance of incident light in visible region. The protection effect of TiO_2 film to active layer by decreasing the transmittance of ultraviolet (350–400 nm) light was investigated through time-dependent absorption measurements under the irradiation of simulated AM 1.5 sunlight. The active layers on the ITO/PEDOT:PSS substrate and ITO/TiO_2 substrate were irradiated under AM 1.5 sunlight, and the absorption spectra were recorded at various time. As shown in Fig. S4 of ESI,† the absorbances decrease gradually along with extending irradiation time. After irradiation of 7 h, 98.86% and 98.00% of initial absorbances are remained for the active layers on the substrates with and without TiO_2 layer, respectively. It directly proves the protection effect of TiO_2 film to active layer by decreasing the transmittance of ultraviolet light. For the annealed TiO_2/ITO, the transmittance decreased on a large scale especially in range of 420–580 nm, probably due to the destruction of ITO film during the high-temperature treatment.[19] In most high-temperature processed TiO_2 based solar cells, thermostable substrate such as FTO was explored instead of ITO, which would bring with low transmittance and conductivity for the electrode. Herein, the utilization of the room-temperature processed nanocrystal TiO_2 layer not only protected ITO from thermal destruction but also enabled the fabrication of solar cells on other thermal sensitive substrates such as polyethyleneterephthalate (PET).[2]

The electronic properties, in terms of energy levels and electron mobility, of the TiO_2 nanocrystal film were also studied. Based on the UPS spectra and absorption coefficient (Fig. S5 and S6 in ESI†), the valence band (VB) and band gap of the TiO_2 nanocrystal film were determined to be 7.0 eV and 3.3 eV respectively, and as a consequence, the conduction band (CB) was calculated to be 3.7 eV. The energy levels of this TiO_2 nanocrystal film were in good agreement with those of other reported TiO_2 ECLs,[18,19] which demonstrated its energy-aligning capability as effective ECL. The electron mobility of the TiO_2 nanocrystal film was estimated by the space charge limited current (SCLC) method (Fig. S7 in ESI†) and the value of 2.7×10^{-3} cm^2 V^{-1} s^{-1} could surpass that of the previously reported anatase TiO_2 nanorods (2.33×10^{-4} cm^2 V^{-1} s^{-1}) measured by the same method.[30] These electronic properties endow the TiO_2 nanocrystal film with effective electron collecting and transporting ability.

In order to illustrate the utilization of the TiO_2 nanocrystal film with favourable morphology, optical and electronic properties, a prove-of-concept inverted OSC has been fabricated which explored the TiO_2 nanocrystal film as ECL (device 1). On the pre-clean ITO substrate, the TiO_2 nanocrystal film was fabricated by spin-coating the dispersion of TiO_2 nanocrystals in ethanol. Without any further treatment on the TiO_2 nanocrystal film, a P3HT:PCBM active layer, a MoO_3 layer and an Ag electrode were deposited successively (for details, please see Experiment section). Fig. 4a showed a FE-SEM cross-section of the device and illustrated the schematic device structure. Device 1 exhibited a satisfying photovoltaic performance with an open circuit voltage (V_{oc}) of 0.59 V, a short-circuit current density (J_{sc}) of 9.27 mA cm^{-2}, a fill factor (FF) of 0.61, and an overall power conversion efficiency (PCE) of 3.35% (best value of 30 devices with an average PCE of 3.11%) respectively under simulated AM 1.5 (100 mW cm^{-2}) sunlight (Fig. 4b). The performance of device 1 was comparable to that of the conventional OSC (device 2 with the structure of ITO/PEDOT:PSS (40 nm)/P3HT:PCBM (210 nm)/LiF (1 nm)/Al (100 nm)) with high-performance PCE of 3.39% (Fig. 4b). This result strongly illustrated the effective electron collection and transport abilities of the nanocrystal TiO_2 layer and the feasibility to explore the TiO_2 nanocrystal film as ECL for OSCs. In addition, a reference inverted OSC

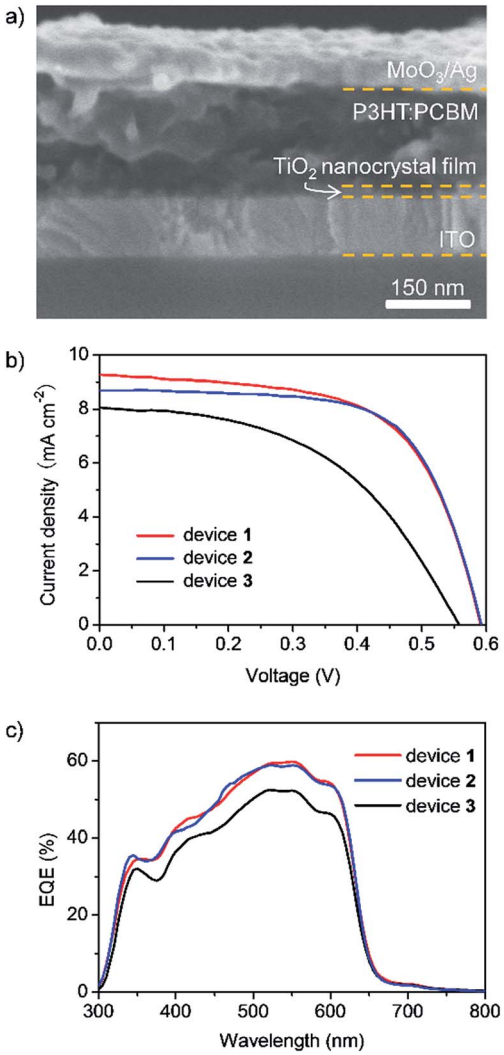

Fig. 4 (a) FE-SEM cross-section image of device 1. (b) Current density *versus* voltage (*J*–*V*) curves of devices 1–3 (with the structures of device 1: ITO/TiO_2 nanocrystal layer (25–30 nm)/P3HT:PCBM (210 nm)/MoO_3 (5.5 nm)/Ag (70 nm), device 2: ITO/PEDOT:PSS (40 nm)/P3HT:PCBM (210 nm)/LiF (1 nm)/Al (100 nm), and device 3: ITO/annealed TiO_2 layer (35 nm)/P3HT:PCBM (210 nm)/MoO_3 (5.5 nm)/Ag (70 nm)). (c) EQE spectra of devices 1–3.

(device 3) with traditionally high-temperature annealed TiO_2 as ECL was fabricated on ITO substrate for comparison. The performance of device 3 gave a reduction on V_{oc},J_{sc}, FF and thus an overall PCE which were 0.56 V, 8.07 mA cm^{-2}, 0.48 and 2.18% respectively (Fig. 4b), due to the optical and electronic alteration of ITO/TiO_2 layers under high-temperature annealing.[19,31] This comparison highlighted the advantage of fabricating TiO_2 nanocrystal film using this method in moderate condition to avoid the undesired high-temperature treatment on TiO_2 ECL.

To gain a deep insight into the effect of TiO_2 nanocrystal film, the external quantum efficiency spectrum (EQE) of device 1 was measured and compared with those of devices 2 and 3. As shown in Fig. 4c, the EQE spectrum of device 1 with TiO_2 nanocrystal film is comparable with that of conventional device 2. The maximum of EQE value is 60% at 555 nm for device 1. In contrast, the EQE spectrum of device 3 with high-temperature annealed TiO_2 film is much lower, and the maximum of EQE value decreases to 52% at 520 nm. The EQE measurements further indicate the effectiveness and advantage of the TiO_2 nanocrystal film fabricated by this annealing-free method.

Conclusion

An extremely convenient and moderate approach to fabricate anatase TiO_2 nanocrystal film as electron collection layer in photovoltaics has been developed. Ultrafine, clean and high-quality anatase TiO_2 nanocrystal dispersion has been pre-prepared in a simple route and spin-coating the nanocrystal dispersion at room temperature provides a well performed TiO_2 nanocrystal layer. It should be noted that, without any further treatments (such as high temperature annealing), the TiO_2 nanocrystal film exhibited favourable morphology, optical and electronic properties, and in consequence was successfully applied as ECL in inverted OSC. This approach has overcome the ugly defect of high-temperature annealing process in traditional fabrication of anatase TiO_2 ECLs. As thin TiO_2 ECLs are broadly used in other thin film solar cells such as inverted hybrid solar cells and planar perovskite solar cells besides OSCs, the annealing-free TiO_2 nanocrystal film has the potential to be employed in other photovoltaic systems and will meet further demands for low temperature processing plastic solar cells.

Acknowledgements

This work was supported by the National Natural Science Foundation of China (61306081, 61176016), Natural Science Foundation of Jilin Province (20130522142JH, 20121801).

Notes and references

1 G. Yu, J. Gao, J. C. Hummelen, F. Wudl and A. J. Heeger, *Science*, 1995, **270**, 1789–1791.
2 F. C. Krebs, *Sol. Energy Mater. Sol. Cells*, 2009, **93**, 394–412.
3 S. H. Park, A. Roy, S. Beaupre, S. Cho, N. Coates, J. S. Moon, D. Moses, M. Leclerc, K. Lee and A. J. Heeger, *Nat. Photonics*, 2009, **3**, 297–302.
4 F. C. Krebs, N. Espinosa, M. Hösel, R. R. Søndergaard and M. Jørgensen, *Adv. Mater.*, 2014, **26**, 29–39.
5 L. Lu, T. Zheng, Q. Wu, A. M. Schneider, D. Zhao and L. Yu, *Chem. Rev.*, 2015, DOI: 10.1021/acs.chemrev.5b00098.
6 R. Steim, F. R. Kogler and C. J. Brabec, *J. Mater. Chem.*, 2010, **20**, 2499–2512.
7 F.-x. Xie, W. C. H. Choy, W. E. I. Sha, D. Zhang, S. Zhang, X. Li, C.-w. Leung and J. Hou, *Energy Environ. Sci.*, 2013, **6**, 3372–3379.
8 M. Graetzel, R. A. J. Janssen, D. B. Mitzi and E. H. Sargent, *Nature*, 2012, **488**, 304–312.
9 C.-Y. Li, T.-C. Wen, T.-H. Lee, T.-F. Guo, J.-C.-A. Huang, Y.-C. Lin and Y.-J. Hsu, *J. Mater. Chem.*, 2009, **19**, 1643–1647.
10 E. J. W. Crossland, N. Noel, V. Sivaram, T. Leijtens, J. A. Alexander-Webber and H. J. Snaith, *Nature*, 2013, **495**, 215–219.
11 K. Lee, J. Y. Kim, S. H. Park, S. H. Kim, S. Cho and A. J. Heeger, *Adv. Mater.*, 2007, **19**, 2445–2449.
12 H. Sun, J. Weickert, H. C. Hesse and L. Schmidt-Mende, *Sol. Energy Mater. Sol. Cells*, 2011, **95**, 3450–3454.
13 A. Hagfeldt and M. Grätzel, *Acc. Chem. Res.*, 2000, **33**, 269–277.
14 A. Karpinski, S. Berson, H. Terrisse, M. Mancini-le Granvalet, S. Guillerez, L. Brohan and M. Richard-Plouet, *Sol. Energy Mater. Sol. Cells*, 2013, **116**, 27–33.
15 H. Hänsel, H. Zettl, G. Krausch, R. Kisselev, M. Thelakkat and H. W. Schmidt, *Adv. Mater.*, 2003, **15**, 2056–2060.
16 M. Liu, M. B. Johnston and H. J. Snaith, *Nature*, 2013, **501**, 395–398.
17 J. T.-W. Wang, J. M. Ball, E. M. Barea, A. Abate, J. A. Alexander-Webber, J. Huang, M. Saliba, I. Mora-Sero, J. Bisquert, H. J. Snaith and R. J. Nicholas, *Nano Lett.*, 2014, **14**, 724–730.
18 K.-L. Ou, D. Tadytin, K. Xerxes Steirer, D. Placencia, M. Nguyen, P. Lee and N. R. Armstrong, *J. Mater. Chem. A*, 2013, **1**, 6794–6803.
19 J.-H. Huang, H.-Y. Wei, K.-C. Huang, C.-L. Chen, R.-R. Wang, F.-C. Chen, K.-C. Ho and C.-W. Chu, *Energy Environ. Sci.*, 2010, **3**, 654–658.
20 Z. Lin, C. Jiang, C. Zhu and J. Zhang, *ACS Appl. Mater. Interfaces*, 2013, **5**, 713–718.
21 H. C. Weerasinghe, P. M. Sirimanne, G. V. Franks, G. P. Simon and Y. B. Cheng, *J. Photochem. Photobiol., A*, 2010, **213**, 30–36.
22 H. Lee, D. Hwang, S. M. Jo, D. Kim, Y. Seo and D. Y. Kim, *ACS Appl. Mater. Interfaces*, 2012, **4**, 3308–3315.
23 D. Liu and T. L. Kelly, *Nat. Photonics*, 2014, **8**, 133–138.
24 K. Wojciechowski, M. Saliba, T. Leijtens, A. Abate and H. J. Snaith, *Energy Environ. Sci.*, 2014, **7**, 1142–1147.
25 B. Conings, L. Baeten, T. Jacobs, R. Dera, J. D'Haen, J. Manca and H.-G. Boyen, *APL Mater.*, 2014, **2**, 081505.
26 H. G. Yang, G. Liu, S. Z. Qiao, C. H. Sun, Y. G. Jin, S. C. Smith, J. Zou, H. M. Cheng and G. Q. Lu, *J. Am. Chem. Soc.*, 2009, **131**, 4078–4083.

27 W.-H. Baek, I. Seo, T.-S. Yoon, H. H. Lee, C. M. Yun and Y.-S. Kim, *Sol. Energy Mater. Sol. Cells*, 2009, **93**, 1587–1591.
28 F. J. Lim, A. Krishnamoorthy and G. W. Ho, *ACS Appl. Mater. Interfaces*, 2015, **7**, 12119–12127.
29 O. Wiranwetchayan, Q. Zhang, X. Zhou, Z. Liang, P. Singjai and G. Cao, *Chalcogenide Lett.*, 2012, **9**, 157–163.
30 Y.-C. Tu, J.-F. Lin, W.-C. Lin, C.-P. Liu, J.-J. Shyue and W.-F. Su, *CrystEngComm*, 2012, **14**, 4772–4776.
31 Ref: the high temperature annealing process leads to a serious degree of In species diffusion between the TiO_2 and ITO films, which lowers the conductivity of ITO and brings quenching centers into TiO_2 layer, thus has a negative effect on the efficiency.